

A pure-carbon ring transistor: The rôle of topology and structure

Gianaurelio Cuniberti^{a)}, Juyeon Yi, and Markus Porto

Max-Planck-Institut für Physik komplexer Systeme, Nöthnitzer Straße 38, 01187 Dresden, Germany

(Dated: March 27, 2002)

We report results on the rectification properties of a carbon nanotube (CNT) ring transistor, contacted by CNT leads, whose novel features have been recently communicated by Watanabe *et al.* [Appl. Phys. Lett. **78**, 2928 (2001)]. This paper contains results which are validated by the experimental observations. Moreover, we report on additional features of the transmission of this ring device which are associated with the possibility of breaking the lead inversion symmetry. The linear conductance displays a “chessboard”-like behavior alternated with anomalous zero-lines which should be directly observable in experiments. We are also able to discriminate in our results structural properties (quasi-one-dimensional confinement) from pure topological effects (ring configuration), thus helping to gain physical intuition on the rich ring phenomenology.

PACS numbers: 05.60.-k, 72.80.Le, 73.40.-c, 81.07.-b

Keywords: Molecular transistors; carbon nanotubes; charge transport.

Carbon materials are at the base of the many molecular electronics achieved goals.¹ The discovery of the C₆₀ molecule² and, later on, of carbon nanotubes (CNTs)³ provided experimentalists with nanometer-scale materials with exceptional electronic and mechanical properties.⁴ The adoption of an individual C₆₀ molecule connected to gold electrodes made possible to measure transistor like features.⁵ In a parallel development, also logic circuits with field-effect transistors based on single CNTs have been probed.^{6,7} In most of the aforementioned experiments, the focus has been centered on carbon-based molecules, C₆₀, single-wall (SW) or multi-wall (MW) CNTs, bridged between bulky leads.

However, CNTs have been also shown useful as wiring elements,⁸ e.g., when employed to enhance the resolution of scanning tunneling microscope (STM) tips.^{9,10} Indeed, in a pioneering experiment published in this jour-

nal, Watanabe *et al.*¹¹ managed to contact a CNT ring to CNT-STM tips. Their apparatus, which is schematically drawn in Fig. 1, realizes a pure-carbon transistor. The two CNT leads, biased by a potential V_{sd} , are the source and the drain for the current flowing through the CNT-ring; the latter is sitting on a surface which fixes the gate voltage to V_g . This system, which is the object of our theoretical investigation, exhibits an interesting variety of effects mainly due to the ring topology and to the underlying carbon nanostructure. Our results are validated by the experiment of Watanabe *et al.*¹¹ but show interesting additional phenomena which should be directly detectable in future experiments.

We treat the transport problem in the system at hand by calculating the transmission t through an armchair (ℓ, ℓ) CNT ring within the Landauer approach.¹² The relation between the Hamiltonian of the system and the transmission¹³ is given by means of the retarded Green function $G^{\text{ring}} = (E + i0^+ - H^{\text{ring}})^{-1}$, where H^{ring} is the ring π electron Hamiltonian. Provided that the system has atomic contacts, one can show that the calculus of the transmission simplifies to

$$t_n(E) = 4 \Delta_{11}(E) \Delta_{nn}(E) \left| G_{1n}^{\text{ring}}(E) / \det(Q) \right|^2, \quad (1)$$

where $\Sigma = \Lambda - i\Delta$ is the semi-infinite armchair (ℓ, ℓ) CNT lead self-energy, $Q = I - \Sigma G^{\text{ring}}$, and I is the unity matrix. Recently, both Λ and Δ have been obtained analytically.¹⁴ We assume that the fixed first lead has an atomic contact to the first ring atom of the upmost circumference line spanned by the second lead. The position of the latter is determined by the second contacted atom $n = 2, \dots, 2c$ (see Fig. 1). The total number of upmost atoms, $2c$, is two times the number of unit cells, c , due to the choice of the armchair tubes. We can span contacts (dashed area in Fig.1) ranging from a single atomic contact to all surface atoms of the CNT leads contacted to the lead.¹⁴ For sake of simplicity we present here only atomic contacts results. The numerical computational task is thus shifted to the calculus of the matrix element

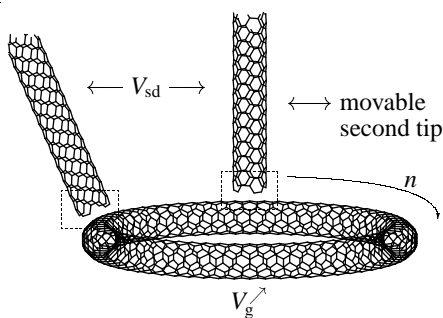


FIG. 1: A pure-carbon ring transistor. The two semi-infinite CNT leads can scan the upper surface of the CNT ring. The latter is supposed to lie on a surface imposing a gate voltage V_g , fixed with respect to the second lead as in Ref. 11. The quality and nature of the contacts (dashed boxes) is discussed in the text.

^{a)}E-Mail: cunibert@mpipks-dresden.mpg.de

of G^{ring} between the two contacted atoms, G_{1n}^{ring} , and the determinant of the matrix Q ; this problem grows as N^4 , $N = 2c\ell$ being the number of atoms in the CNT ring.

Fig. 2 shows the dependence of the linear transmission on the position of the second lead, n , and on the gate voltage, V_g . The latter is in units of the hopping parameter, $\gamma = 2.6$ eV, between neighboring carbon atoms. The number of unit cells considered in the ring is $c = 16$ (i.e., 32 upmost atoms) and the size of both the ring and lead tubes are fixed by imposing $\ell = 4$. The density plot appears quite complex and reflects the presence of van Hove singularities in the system (see the insets of Fig. 2) but certain regularities emerge. At a fixed gate voltage the position dependence of the transmission exhibit a “chessboard”-like behavior. The latter is broken for particular values of the gate voltage where zeros in the transmission occur. This is a typical topological effect which has been shown analytically for one-dimensional rings.¹⁵ These zeros are a direct consequence of the breaking of the inversion symmetry and are either due to destructive interference events or due to the matching between the gate voltages and particular eigenvalues of the system.¹⁵

With the knowledge of the transmission function $t_n(E)$, it is straightforward to evaluate the I - V characteristics by applying the standard formalism based on the scattering theory of transport¹⁶

$$I_n = \frac{2e}{h} \int_{-\infty}^{\infty} dE t_n(E) [f_L(E) - f_R(E)]. \quad (2)$$

Here $f_{L,R}(E) = \{\exp[(E - \mu_{L,R})/k_B T] + 1\}^{-1}$ is the Fermi function, μ_L and μ_R are the electrochemical potentials of

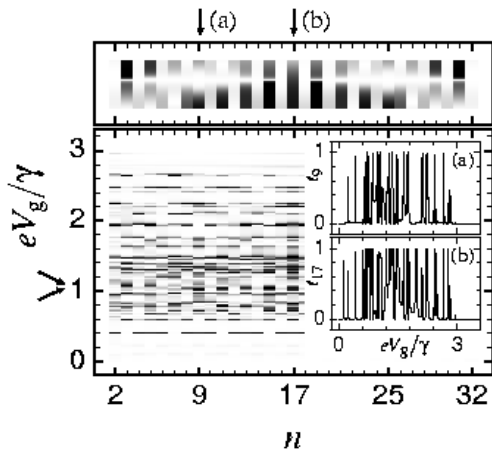


FIG. 2: Density plot of the linear transmission $t_n(E \rightarrow 0)$ as a function of the position n and of the gate voltage V_g . In this scale white corresponds to 0 and black to 1. In the insets, the explicit gate voltage dependence of the transmission is shown for (a) $n = 9$ (90 deg) and for (b) $n = 17$ (180 deg). The top panel illustrates a blow up of the transmission in a small gate voltage window (indicated by tilted arrows) where zeros in the transmission occur (a better resolution figure is available upon request).

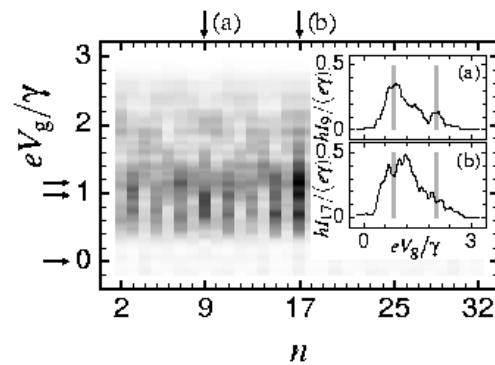


FIG. 3: Density plot of the current (STM images) at $V_{sd} = 1$ V as a function of the position n and of the gate voltage V_g . In this scale white corresponds to no current and black to maximum current. The horizontal arrows refer to the three gate voltages $V_g = 0, 2.5, 3$ V considered in Ref. 11 (Fig. 3) for producing the STM images. The two insets show the details of the gate voltage dependence for the two configuration (a) $n = 9$ (90 deg) and (b) $n = 17$ (180 deg), respectively. The gray bars indicate the regions where $I_9 \geq I_{17}$ (a better resolution figure is available upon request).

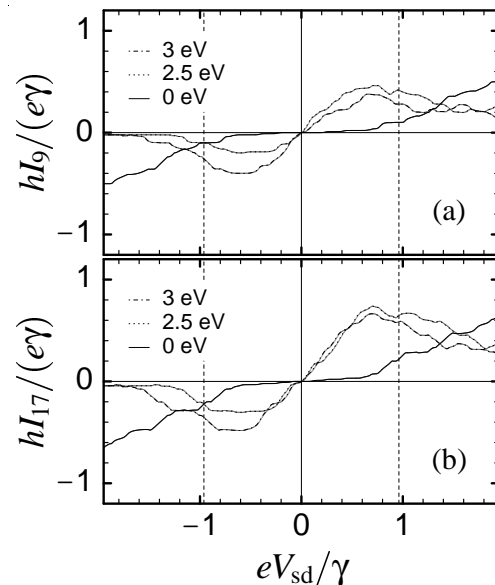


FIG. 4: Lead-orientation dependent rectification, for three different gate voltages $V_g = 0, 2.5, 3$ V, illustrated (a) for the 90 deg configuration and (b) for the inversion symmetric one.

the two metal electrodes, whose difference is fixed by the applied bias voltage V_{sd} . The room temperature ($k_B T \simeq 26$ meV) will be considered in the numerical results, in order to keep consistency with the experiment.¹¹

Fig. 3 displays the current at $V_{sd} = 1$ V for different positions of the second CNT tip and for different gate voltages. This quantity has been used to produce the STM images in Ref. 11, where three different values of gate voltages have been considered (here indicated as the

three horizontal arrows in Fig. 3). The inversion symmetric configuration shows a marked current density for wide ranges of gate voltages, apart from two small intervals around 2.7 V and 5.8 V, respectively. At these voltages, transport is much more favored in the lobes of the ring which, for the choice of our size, emerge at the 90 deg configuration (see the gray regions in the inset of Fig. 3).

Fig. 4 (b) shows the I - V characteristics for the inversion symmetry position of the second lead (180 deg). The rectification effect given by the action of the gate potential are due to the finiteness of the ring band which, under a gate shift, is pushed in a region without states. Different is the situation in the 90 deg configuration (Fig. 4 (a)), where no marked asymmetry in the gated I - V curves can be detected. The vertical dashed lines in Fig. 4 indicate the range of bias voltages investigated in Ref. 11. Our calculations outside this region show dominant negative differential conductance effects given by

the action of the gate voltage. The latter is responsible for shifting the CNT ring band in a energy region where much fewer states are available for transport.

More detailed experimental studies on the evolution of the differential conductance with a broken inversion symmetry might probe the striking scenario of the dependence of the STM images on both position and gate voltage. Moreover, this pure-carbon system, where electron transfer between leads and molecule is approximately negligible, may turn out as the best playground to study the effect of contacts on the overall transport measurement.

Acknowledgments

GC research at MPI is sponsored by the Schloëßmann Foundation.

-
- ¹ R. F. Service, *Science* **294**, 2442 (2001).
² H. W. Kroto, J. R. Heath, S. C. O'Brien, R. F. Curl, and R. E. Smalley, *Nature* **318**, 162 (1985).
³ S. Iijima, *Nature* **354**, 56 (1991).
⁴ M. S. Dresselhaus, G. Dresselhaus, and P. C. Eklund, *Science of fullerenes and carbon nanotubes* (Academic Press, Inc., 1996).
⁵ H. Park, J. Park, A. K. L. Lim, E. H. Anderson, A. P. Alivisatos, and P. L. McEuen, *Nature* **407**, 57 (2000).
⁶ A. Bachtold, P. Hadley, T. Nakanishi, and C. Dekker, *Science* **294**, 1317 (2001).
⁷ T. Rueckes, K. Kim, E. Joselevich, G. Y. Tseng, C.-L. Cheung, and C. M. Lieber, *Science* **289**, 94 (2000).
⁸ N. Yoneya, E. Watanabe, K. Tsukagoshi, and Y. Aoyagi, *Appl. Phys. Lett.* **79**, 1465 (2001).
⁹ C. L. Cheung, C. M. Lieber, and J. H. Hafner, *Nature* **398**, 761 (1999).
¹⁰ S. S. Wong, E. Joselevich, A. T. Woolley, C. L. Cheung, and C. M. Lieber, *Nature* **394**, 52 (1998).
¹¹ H. Watanabe, C. Manabe, T. Shigematsu, and M. Shimizu, *Appl. Phys. Lett.* **78**, 2928 (2001).
¹² R. Landauer, *IBM J. Res. Develop.* **1**, 223 (1957), reprinted in *J. Math. Phys.* **37**, 5259 (1996).
¹³ D. S. Fisher and P. A. Lee, *Phys. Rev. B* **23**, R6851 (1981).
¹⁴ G. Cuniberti, G. Fagas, and K. Richter, *Chem. Phys.* (in print).
¹⁵ J. Yi, G. Cuniberti, and M. Porto, (unpublished).
¹⁶ S. Datta, *Electronic Transport in Mesoscopic Systems* (Cambridge University Press, Cambridge, 1999).